

Measurement of the Fast Neutron
Detection Efficiency for a
NaI(Tl) Scintillator

Prepared by
Kendrick L Killian

ARTHUR LAKES LIBRARY
COLORADO SCHOOL of MINES
GOLDEN, COLORADO 80401
CLOSED RESERVE

ProQuest Number: 11016539

All rights reserved

INFORMATION TO ALL USERS

The quality of this reproduction is dependent upon the quality of the copy submitted.

In the unlikely event that the author did not send a complete manuscript and there are missing pages, these will be noted. Also, if material had to be removed, a note will indicate the deletion.



ProQuest 11016539

Published by ProQuest LLC (2019). Copyright of the Dissertation is held by the Author.

All rights reserved.

This work is protected against unauthorized copying under Title 17, United States Code
Microform Edition © ProQuest LLC.

ProQuest LLC.
789 East Eisenhower Parkway
P.O. Box 1346
Ann Arbor, MI 48106 – 1346

A thesis submitted to the Faculty and the Board of Trustees of the Colorado School of Mines in partial fulfillment of the requirements for the degree of Master of Science (Physics).

Golden, Colorado

Date 12/20, 1978

Signed: Kendrick Hillman

Approved: H. Leil

Golden, Colorado

Date 12/20, 1978

H. Schweingart

ABSTRACT

A NaI(Tl) detector may be used as a high efficiency neutron detector through the use of the fast neutron produced reaction $^{127}\text{I}(n,n')$. The inelastic scattering excites the ^{127}I to its 57 keV first excited state and the crystal absorbs the subsequent deexcitation gamma. The interaction length for neutron detection was measured for neutron energies of 2.8 Mev and 14.8 Mev. These interaction lengths were, at 2.8 Mev $.0079 \pm .0009 \text{ cm}^{-1}$ and at 14.8 Mev $.005 \pm .0005 \text{ cm}^{-1}$.

TABLE OF CONTENTS

Introduction	1
Proceedure	6
Results	13
Table 1	
Sample Data and Results	19
Figures	20
Appendix A	
Detection Efficiency of a Detector Near a Point Source.	30
Appendix B	
Determination of the Efficiency of the Ge(Li) Detector	33
References	35

LIST OF FIGURES

	page
Intrinsic Efficiency as a Function of Neutron Energy for an Organic Scintillator	20
Level Diagrams for The Lowest Levels of ^{127}I and ^{22}Na	21
Pulse Height Spectra of Interest from a NaI(Tl) Scintillator	22
Experimental Set Up	23
Spectrum of In Sample After Neutron Bombardment	24
Typical NaI(Tl) Neutron Response	25
57 keV Peak and Two "Best Fit" Backgrounds	26
Plot of Deuterated-Titanium Thick Target Neutron Yield and Experimentally Measured Yields	27
Interaction Length for the Production of the First Excited State in ^{127}I	28
Neutron Cross Sections for Several Reactions Used in Neutron Detection	29

Acknowledgements

I would like like to thank the U.S. Geologic Survey for which this work was done under USGS Grant #14-08-0001-g-548. I must also thank Dr. F.E. Cecil for his guidance and M. Rymes for his help in making the measurements. Last I want to express my appreciation to my family and friends who offered their invaluable assistance and support in the preparation of this thesis.

The detection of neutrons has become an important part of several areas of pure and applied physics. The reason for the neutron's usefulness is its lack of charge. This lack of charge enables a neutron to interact with the atomic nucleus without being affected by either the nuclear electric field or the electronic charge distribution.

In applied physics, neutron induced reactions have proven to be very useful in non-destructive elemental analysis. A variation on this idea is to detect and assay Uranium in situ by neutron induced fission (1). The fissions are detected by counting the delayed fission neutrons. Counting the delayed neutrons offers the advantage that the neutron source can be pulsed, while keeping the background to a minimum. Furthermore, the half life of the delayed neutrons ranges from several milliseconds to seconds thus producing a significant signal in a reasonably short counting period. This seems to be very promising for borehole logging as neutron sources can be made small enough to fit down a borehole.

In basic nuclear physics, neutron spectroscopy has become one of the 8 fundamental nuclear research tools. An example of this is the study of proton rich nuclei by the use of the ($^3\text{He}, n$) reaction (2). The escaping neutron carries away the energy excess between the incident energy

and that of the final nuclear state. Thus, by determining the time needed for a neutron to traverse a known distance, the neutron's energy can be found and the energy left in the nucleus can be determined.

The problem with neutron detection is, however, that the neutron's lack of charge makes it difficult to detect because all particle or gamma detectors ultimately detect the passage of a charged particle. As a result a neutron can only be detected when it participates in some nuclear reaction.

There are several nuclear reactions used in the detection of neutrons. Probably the most basic of these reactions is simple elastic scattering of the neutron off of a Hydrogen nucleus in an organic scintillator and the subsequent detection of the recoiling proton. Problems arise in the fact that the recoiling proton can have any energy from zero up to the incident neutron's full energy. When the number of counts is plotted versus energy, a mono-energetic neutron source produces a plateau rather than a peak. Since an organic scintillator detects gamma radiation mainly by Compton scattering, which also produces a counts versus energy plateau, further processing of the data by time of flight analysis or pulse shape discrimination is virtually mandatory to eliminate

background (2). On the plus side is that an organic scintillator can count as many as 10% of the neutrons entering the detector, including count loss due to the discriminator needed to reject electronic noise (Figure 1):

Other nuclear processes like $\text{He}(n,p)t$ and $\text{Li}(n,)t$ reactions have been used because the final products are charged and are easily detected. When the counts from these reactions are plotted in the usual manner, a well defined peak is present and the shift of the peak from the known Q value for the reaction is the energy of the incoming neutron. The main problem with these detectors is that the neutron detection efficiency drops rapidly with increasing neutron energy. Typically, at 2.5 MeV the efficiency of these neutron spectrometers, as quoted by Ortec for their systems, has dropped to 3×10^{-6} and 7×10^{-7} for the two reactions respectively (3):

There are also many nuclear reactions that are useful as integrating flux monitors at certain energies. Typical of these is the $^{63}\text{Cu}(n,2n)$ reaction which subsequently beta plus decays providing a useful monitor for 14. Mev neutrons. The final activity of one of these monitors is dependent only on the time of bombardment by the neutrons and the average neutron flux. However, as with any detector whose output is some quantity integrated over time, there is no

way to determine the length or magnitude of any perturbation in the measured quantity and there is no way to do real time measurements.

In the present work, we investigate the usefulness of inelastic scattering as a method of neutron detection. After the neutron scatters off of the target, the affected nucleus will return to the ground state almost exclusively by emitting a gamma ray. This gamma ray can then be detected by the use of a scintillator. In the present case the target nucleus is the ^{127}I in a NaI(Tl) crystal. Not only is the crystal the target but it is the scintillator.

As can be seen from Figure 2, ^{127}I has its first excited state at 57 keV. This excited state gamma decays with a 2 nsec half life back to the ground state (4). The 57 keV gamma ray is very convenient as a detection gamma because of its low energy. At these low energies the photo-electric absorption coefficient for a NaI(Tl) crystal has a value of 30 cm^{-1} , which is much larger than the Compton scattering coefficient which has a value of $.5\text{ cm}^{-1}$ (5). This means virtually all of the gammas produced will appear in the full energy peak. Also, since the range of a low energy gamma in a medium or high Z material is very short, extraneous peaks from external sources can be shielded against with a minimum of material.

Although inelastic scattering appears to be a viable method of neutron detection, it has been neglected in the past. In the 1950's and 60's, NaI(Tl) crystals were used in neutron scattering experiments to determine the excited states of Na and I, and some measurements of the scattering cross section were made using a NaI(Tl) crystal as a target (6), (7), (8). However no reference of the use of a NaI(Tl) crystal as a primary neutron detector was found.

The most complete data on the inelastic neutron scattering cross section for ^{127}I gives values for neutron energies up to 1.2 MeV (9). Using the value of .26 barns for the cross section at 1.2 MeV, and the density of NaI, it was determined that a 1 cc cube of NaI(Tl) has a probability of detecting a neutron given by:

$$1) \quad Pd = \rho (1\text{cm}) \sigma \frac{(6.02 \times 10^{23} \text{ I/mole NaI})}{(150 \text{ gm/mole NaI})} ,$$

where σ is the cross section for the production of the 57 keV gamma from ^{127}I and ρ is the density of NaI in gm/cm³. This indicates that a NaI(Tl) crystal of a common commercial size, such as 3" by 5", should have a fast neutron detection efficiency of 3 %.

Since neutron scattering data is lacking for energies above 1.2 MeV, measurements of the scattering cross sections above this value were needed to increase the usefulness of a

NaI(Tl) neutron detector. Specifically, measurements at 2.8 MeV and 14.8 MeV are needed because these are the energies of the neutrons produced by the d-d and d-t fusion reactions. These reactions have gained use as neutron producing reactions because they are readily produced in small Cockcroft-Walton accelerators.

Procedure

The efficiency of the NaI(Tl) crystal as a neutron detector was obtained by simultaneous measurement of the yield for the 57 keV gamma from ^{127}I and the neutron flux as determined by some other reaction whose cross section is known. For 2.8 MeV neutrons the standard was the $^{115}\text{In}(n,n')$ isomeric transition. The cross section is large compared to other reactions at this energy, while the 4.5 hour half life was still short enough to provide a significant signal to noise ratio. At 14.8 MeV two reactions were used. The first was $^{63}\text{Cu}(n,2n)$ which subsequently beta plus decays and allows detection of the .511 MeV annihilation gamma ray. The second reaction was $^{27}\text{Al}(n,p)$ which beta decays back to ^{27}Al and 80% of the time gives off a .84 MeV gamma.

The neutron flux being measured by a NaI(Tl) detector was independently determined by measuring the activity of the standard (Al, Cu, In) following the completion of the

bombardment. Starting with the differential equation it is easily shown that the number of radioactive nuclei present in a sample at the end of a bombardment with neutrons from a point source is:

$$2) \quad N^* = R_n P(N^*) = \frac{R_n \cdot N_t \cdot \sigma \frac{t_b}{\ln 2}}{4 \pi \cdot R_1 \cdot R_2} \cdot (1 - 2^{-t_b/t_{1/2}}),$$

where

R_n is the neutron production rate
 N_t is the number of target atoms
 σ is the reaction cross section
 $t_{1/2}$ is the excited nuclei's half life
 t_b is the bombardment time
 R_1 and R_2 are the distances from the neutron source to the front and back of the sample.

The $1/(4 \pi R_1 \cdot R_2)$ term comes from the integration, in the small angle approximation, of the $1/r^2$ flux over a small sample of constant area and negligible radius. The number of deexcitation gamma rays detected is:

$$3) \quad D = 2^{-t_w/t_{1/2}} (1 - 2^{-t_c/t_{1/2}}) \cdot N^* \cdot (br \cdot \epsilon \cdot s),$$

where

t_w is the time between the end of bombardment and the start of counting
 t_c is the count time
 br is the appropriate branching ratio
 ϵ is the detector's efficiency
 s is the samples self absorption.

By combining equations 2 and 3, the neutron production rate, R_n , can be written as:

$$4) \quad R_n = \frac{D \cdot 2^{t_w/t_{1/2}}}{(P(N^*) \cdot (1 - 2^{-t_c/t_{1/2}}) \cdot br \cdot \epsilon \cdot s)}$$

The interaction length for the NaI(Tl) detector was defined in a manner similar to the gamma ray absorption coefficient in that the number detected is proportional to the number entering a thin layer. As a result a detector of area A_d and thickness L_d exposed to a plane parallel neutron flux F_n , will detect N_d neutrons where

5) $N_d = N_n \cdot A_d \cdot \lambda \cdot L_d$ and λ is the neutron interaction length. The detectors actually used were cylindrical and it was assumed that they were thin enough that the flux reaching the rear of the detector is not significantly affected by absorption, and that the neutron source is a point, the neutron interaction length λ is:

$$6) \lambda = \frac{D_r \cdot R_d \cdot R_d' \cdot 4\pi}{V_d \cdot R_n \cdot t_b \cdot (1+Ct)}$$

$$= \frac{D_r \cdot R_d (1 + R_d/L_d) \cdot 4\pi}{V_d \cdot R_n \cdot t_b \cdot (1+Ct)}$$

V_d is the volume of the crystal = $L_d A_d$
 R_d and R_d' are distances to the front
and back of the NaI(Tl)
and Ct is a correction term coming from
the integration of r over a large
radius cylinder. (see appendix A)

The difference between this neutron interaction coefficient and the gamma ray absorption coefficient stems from the fact that the neutron's inelastic scattering is not an absorptive process. Since, at high energies, the neutron will scatter mainly in the forward direction, the neutrons

will not be removed from the beam. This means that, ignoring other reactions, the number of neutrons detected by a larger detector will still be approximately the flux times the interaction coefficient. However, this is complicated by the fact that neutrons are absorbed by other reactions. As a result, the neutron flux in the detector will decrease exponentially; however the coefficient of this decrease will only be weakly dependent on the inelastic scattering which leads to the neutrons detection. This is in direct contrast to gamma detection in which detection of the photon either changes the photons energy or removes it entirely. Thus, the number of neutrons detected will go as $\frac{\lambda}{\beta} (1-e^{-\beta L})$ where β is the absorption length, rather than the familiar $(1-e^{-\lambda L})$:

Since neutron detection is a property of the NaI(Tl) crystal and not of a particular NaI(Tl)-photomultiplier combination, the first measurement was to check the efficiency of the optical coupling between these elements. This was done by placing a commercially calibrated gamma source a known distance from the scintillator. The measured number of counts in the photopeak was then compared to the number expected, knowing the source strength, the photopeak to total ratio, and the total detection efficiency for that sized detector at the given source distance. This yielded

photopeak efficiencies of 89%, 98%, and 78% for the three detectors used. This coupling parameter could then be used to correct the measured 57 keV yield.

The detector efficiency and the self absorption of the activation sample were then measured. The activity of the standard samples were measured using the CSM Nuclear Physics laboratory's Ortec Ge(Li) detector and the data recorded with a Tracor Northern multichannel analyzer. As seen in equation 4) the absolute efficiency of the Ge(Li) detector is needed to calculate the number of activations in the standard sample. This efficiency was measured using the commercially calibrated ^{133}Ba , ^{22}Na , ^{54}Mn sources. The Ba has gammas of 81, 276, 303, 356, and 384 keV. These energies not only bracket the ^{115}In 336 keV deexcitation energy allowing the mentioned calibration, but the 81 keV gamma, in conjunction with the Ba X-ray, is useful in calibrating the system for the 57 keV ^{127}I gamma. The usefulness of the radioactive Barium source is evident when the ^{133}Ba and the ^{127}I spectrum in Figure 3 are compared. The ^{22}Na source was used to calibrate the Cu target because both beta plus decay. The ^{54}Mn has an 835 keV gamma which compares well with the ^{27}Al 840 keV energy.

For most of the 14.8 MeV runs the standard sample was placed far enough from the Ge(Li) detector that it approximated a point source, however, this was not possible for the In sample because of low count rates. Thus, an average was taken over the detector face, details of which are described in Appendix B. The absorption coefficient was measured by placing the standard sample in front of the calibrated source and measuring the attenuation. The self absorption was calculated from the absorption coefficient which compared well to the first approximation of 1/2 the measured attenuation.

The work described up to this point was simply preparation for the actual measurements of the NaI(Tl) neutron detection efficiency. The remaining work to be described is this measurement process. The experimental setup is sketched in Figure 4.

These calibration runs were made using the CSM Physics Department's two Cockroft-Walton accelerators which accelerate a Deuterium beam against either a Deuterium-Titanium target or a Tritium-Titanium target. Since the neutron production from these reactions is nearly isotropic, the sample and the NaI(Tl) detector were placed close enough to the beam target to maximize the neutron flux. Due to the number of X-rays produced by the

accelerators, the samples were placed far enough away to allow for adequate shielding. The activation samples were known to be thin; that is, the number of neutrons removed from the flux was small. This allowed the sample to be placed directly in front of the NaI(Tl) crystal without affecting the results.

The tritiated target was placed in a Kaman Nuclear accelerator. This machine accelerates a several hundred μ A beam of D²⁺ from a Penning Ion source through 90 kV. The deuterated target was placed in a Texas Nuclear accelerator because of its higher accelerating voltage (150 kV), its R-F ion source which produces a nearly fully ionized beam, and because the accelerator has never been used with a tritiated target. The Kaman accelerator was initially used for the 2.8 MeV runs, however, the data showed an abnormally large scatter. This phenomenon was best explained by random changes in the operating conditions affecting the average neutron energy because of Tritium contamination. This data was not used in the final analysis although the interaction length calculated from this data is consistent with the final results.

The data was collected by monitoring the NaI(Tl) crystal with the MCA during activation, which usually lasted approximately 25% of the half life of the standard nuclide.

During the 2.8 MeV runs the neutron count was monitored every 500 s to help maintain a constant yield over the long run. The data was typed out of the analyzer while the target sample was moved to the Ge(Li) detector and the system set up. The sample was counted for about one to two half lives. Figure 3b shows the spectra from a typical run. Note the presence of the 57 keV and 202 keV lines from I while the other possible lines indicated by the level diagrams for ^{22}Na and ^{127}I (Figure 2) are not visible. A sample spectrum from the Ge(Li) detector is shown in Figure 5. This spectrum is from the In sample. The 336 keV gamma from the isomeric transition and the 417 keV gamma from the $^{115}\text{In}(n,\gamma)$ reaction are prominent. At these low energies the photopeak efficiency of the Ge(Li) detector is high enough to give an acceptably small statistical error even with a small number of activations.

Results

Table 1 shows the data and results from both a 2.8 MeV and a 14.8 MeV measurement. The error involved in the calculations is dominated by the error resulting from the subtraction of the background from the 57 keV peak. The background was very sensitive to the type and amount of shielding, as would be expected due to the neutron scattering and the copious production of X-rays by the

Cockroft-Walton accelerator. Another concern is the energy resolution of the NaI(Tl) detector. The spectrum shown in Figure 6 is a typical spectrum obtained in the calibration runs. Comparing this spectrum with the one shown in Figure 3b, it is obvious that any increase in resolution decreases the problem with background. These factors meant that the background was most efficiently subtracted by plotting the data points on log-log or semi-log paper and by hand drawing in a reasonable background. The background was then read from the graph and subtracted from the data on a point by point basis. Figure 7 shows one of the runs plotted with two "best" fit backgrounds.

The error in this method of background determination was investigated for the run depicted in Figure 7. The difference between the two determinations of a reasonable background was 8%, while the error between the best fit and a simple trapezoidal background was 15%. This indicates the uncertainty in any single interaction length is a random error of about 10%. This conclusion is confirmed by the standard deviation for the five 2.8 MeV and the four 14.8 MeV interaction lengths. The final interaction lengths and their standard deviations were calculated to be $.0079 \pm .0009$ cm⁻¹ at 2.8 MeV and $.0050 \pm .0005$ cm⁻¹ at 14.8 MeV.

Several things were done to verify that the experimentally determined interaction lengths were in fact reasonable. The first check was done by measuring the interaction length for neutrons from the CSM 2 Curie PuBe source. The PuBe neutron spectrum is a continuous distribution from approximately 1 MeV up to 10 MeV. Since the NaI(Tl)'s response to fast neutrons varies only a factor of two for energies from 1 MeV to 15 MeV, the response to the PuBe source should be approximately its response to the average neutron energy from the PuBe source. As a result the interaction length for the PuBe source should be between those for the two fusion reactions.

The output of the PuBe source was measured to be 1.6×10^6 neutrons /Curie. (The output of a PuBe source seems to be dependent on factors relating to its construction, thus the yield varies between sources.) The interaction length for the PuBe spectrum was calculated to be $.0065 \pm .0011$ cm⁻¹, which compares well with the two established lengths.

The next check was to use a 2x2 NaI(Tl) crystal as a flux monitor to measure the D-D reaction yield at several energies. The CSM accelerators use hydrogenated Titanium targets that are thick enough to stop the incoming Deuterium. As a result the thick target yield was the yield

that was measured. This yield is well known due to its importance in doing neutron activation studies with most small accelerators. The calculated yields were corrected for the anisotropic behavior of the neutron yield from a thick target at 150 keV beam energy using measured data on its angular distribution (10). The data was then compared to the known low energy yield. See Figure 8.

There was a problem with interpreting the yield data because the target used was donated to the CSM Physics department, and the loading of the target was unknown. Despite this uncertainty the data obtained was first plotted as if the target were loaded with the same .25 mg/cm as assumed on the graph. A line, shown as the dotted line on the graph, could then be drawn through the tail of the known curve and through the center of the cluster of measured points. However, this completely ignores the trend line presented by our data.

Assuming that the points all can be shifted up or down on the graph, which is equivalent to multiplying all the data by a constant factor. This constant is the correction for the difference between the actual target loading and the loading used for the reference curve. The points were dropped until a straight line running through the data points intersected the known curve. This resulted in a

reduction of the magnitude of the data by a factor of about 3, which represents an actual loading of $.75 \text{ mg/cm}^2$.

The solid curve on Figure 8 is a smooth curve drawn through the known curve and the reduced data points.

The final check of the consistency of the data was made by comparing the present work with the previously measured cross section curves. There is nothing that prevents a significant portion of the measured 57 keV gammas from being produced as a nucleus cascades down from a higher excited state. This possibility was dismissed because the branching ratios for the higher excited states, as shown in Figure 2, indicate that only 6% of the nuclei in the 202 keV excited state will produce 57 keV gammas, while the branching ratios from higher states are generally smaller. The recorded spectrum shows that the number of 202 keV decays is significantly smaller than the number of 57 keV decays and the higher states are absent altogether. Thus as an upper bound, the number of 57 keV gammas produced as a by product of excitations of the ^{127}I nucleus to a higher excited state should produce no more than a 6% error. Figure 9 shows the neutron interaction length derived from the cross section data, as given by VanLoef and Lind (9), along with the interaction lengths calculated in the present work.

The important cross sections for the other major methods of neutron detection are compared to the cross sections for the production of the 57 keV gamma ray by ^{127}I in Figure 10. One advantage of the NaI(Tl) crystal as a fast neutron detector is the relatively large cross section for the $\text{I}(n,n')$ reaction. In addition, the density of ^{127}I in a NaI(Tl) crystal is high enough that large total efficiencies can be obtained. Another advantage is that the ^{127}I reaction is not sensitive to slow neutrons. This can be an asset when a thermal neutron background, such as that produced by air scattering, is a problem.

As a result of this work the NaI(Tl) neutron detector should be a useful tool in the detection of neutrons. This detection method presents real advantages when real time neutron flux monitoring is desired or when a high sensitivity fast neutron detector is needed. Most nuclear physics laboratories have several NaI(Tl) detectors, thus these detectors would make an inexpensive addition to their neutron detection capabilities.

TABLE 1
SAMPLE DATA AND RESULTS

No. of sample decays	D	2.8 Mev run 710	14.8 MeV run 303
Ge(Li) detector efficiency	ϵ	.803%	.0431%
Time of bombardment	t_b	3500 S	180 S
Cooling Time	t_w	2040 S	90 S
Count time	t_c	3000 S	300 S
Detector area and length	A_d L_d	4.9577 cm ² 5.82 cm	6.377 cm ² 5.1 cm
Distance to sample	R_s	2.9 cm	5.27
distance to detector	R_d	3.3 cm	110 cm
No. of 57 keV counts	D_I	1.84×10^6	18600
sample cross section, σ half-life, # of atoms, $t_{1/2}$ branching ratio, and N_T self absorption	p_r S	.36 barns 4.5 hours 7.11×10^{22} .95 88% escaping	.4 barns 9.9 min 1.53×10^{23} 2 83% escaping

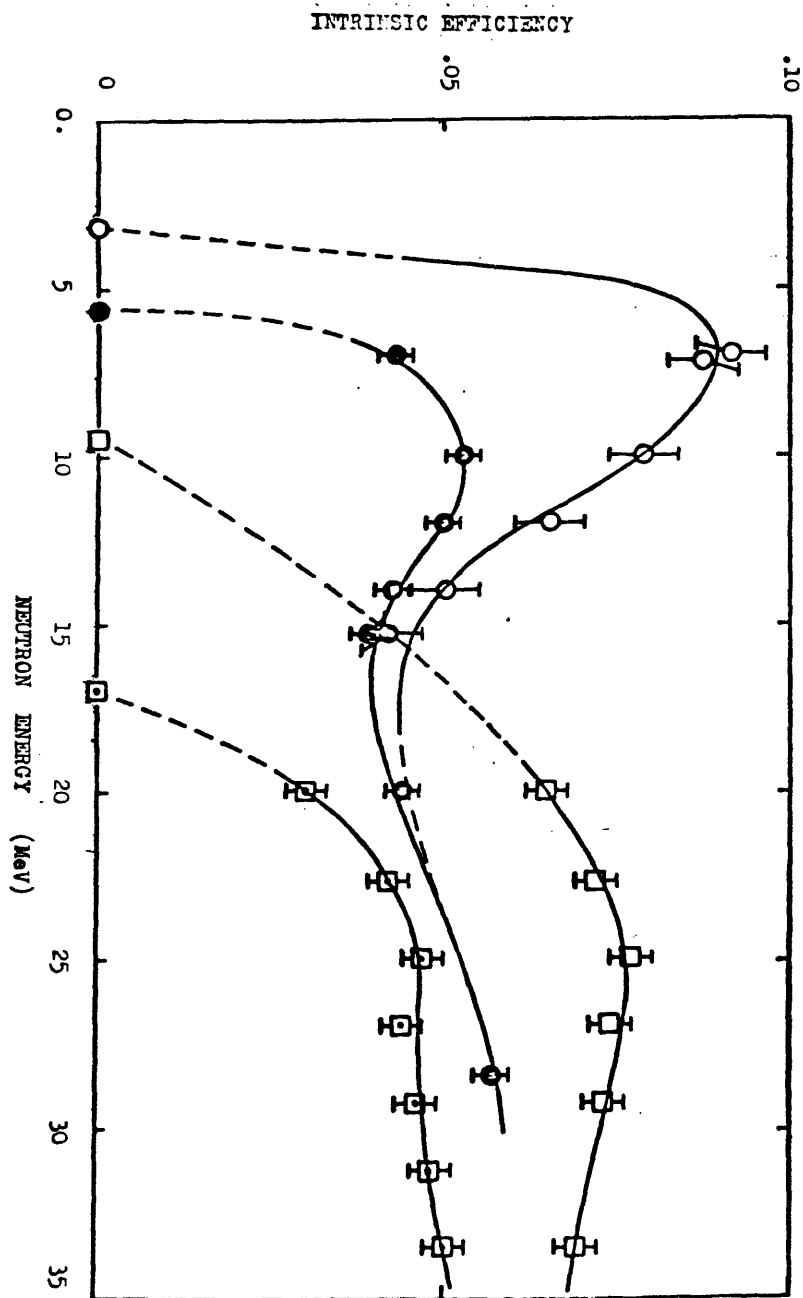


Figure 1 Intrinsic Efficiency as a Function of Neutron Energy for an Organic Scintillator. Four efficiency curves are shown with the associated discriminator energy setting. (2)

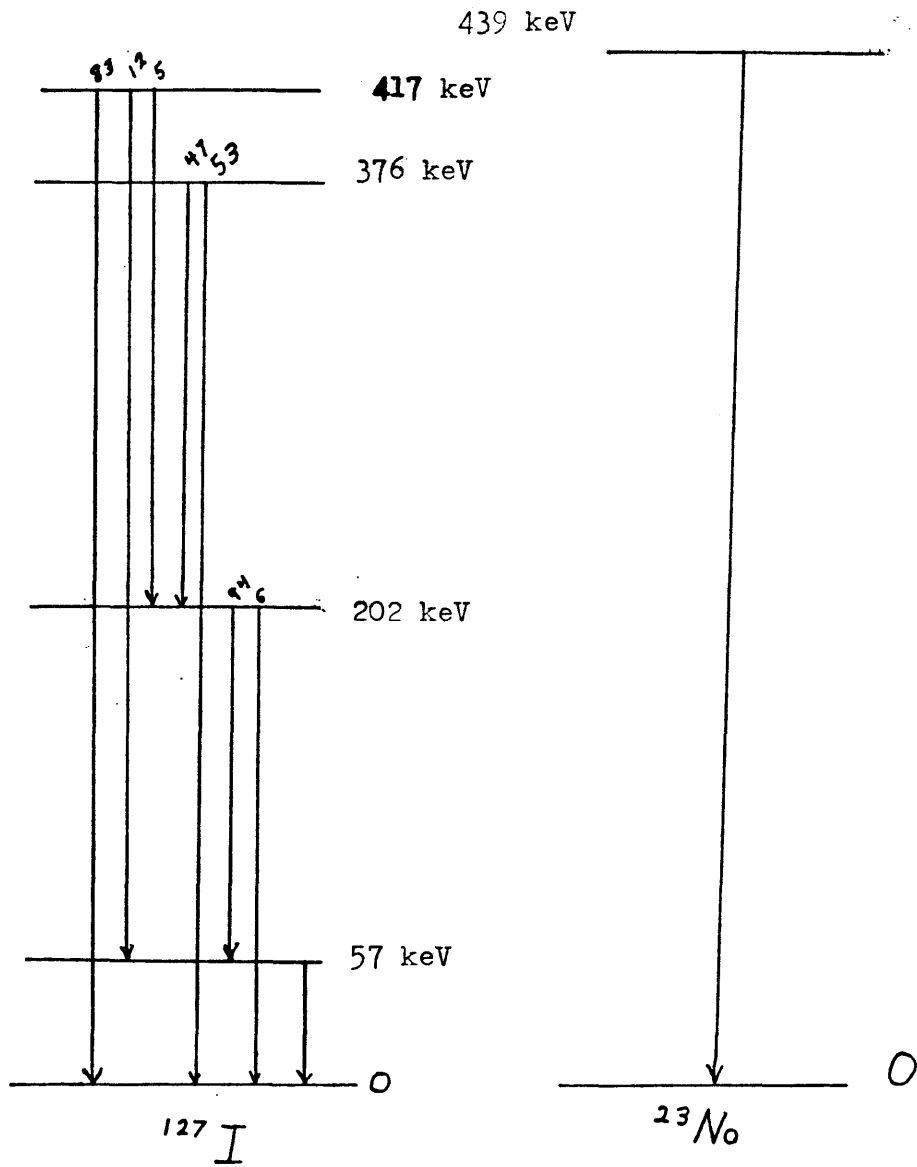
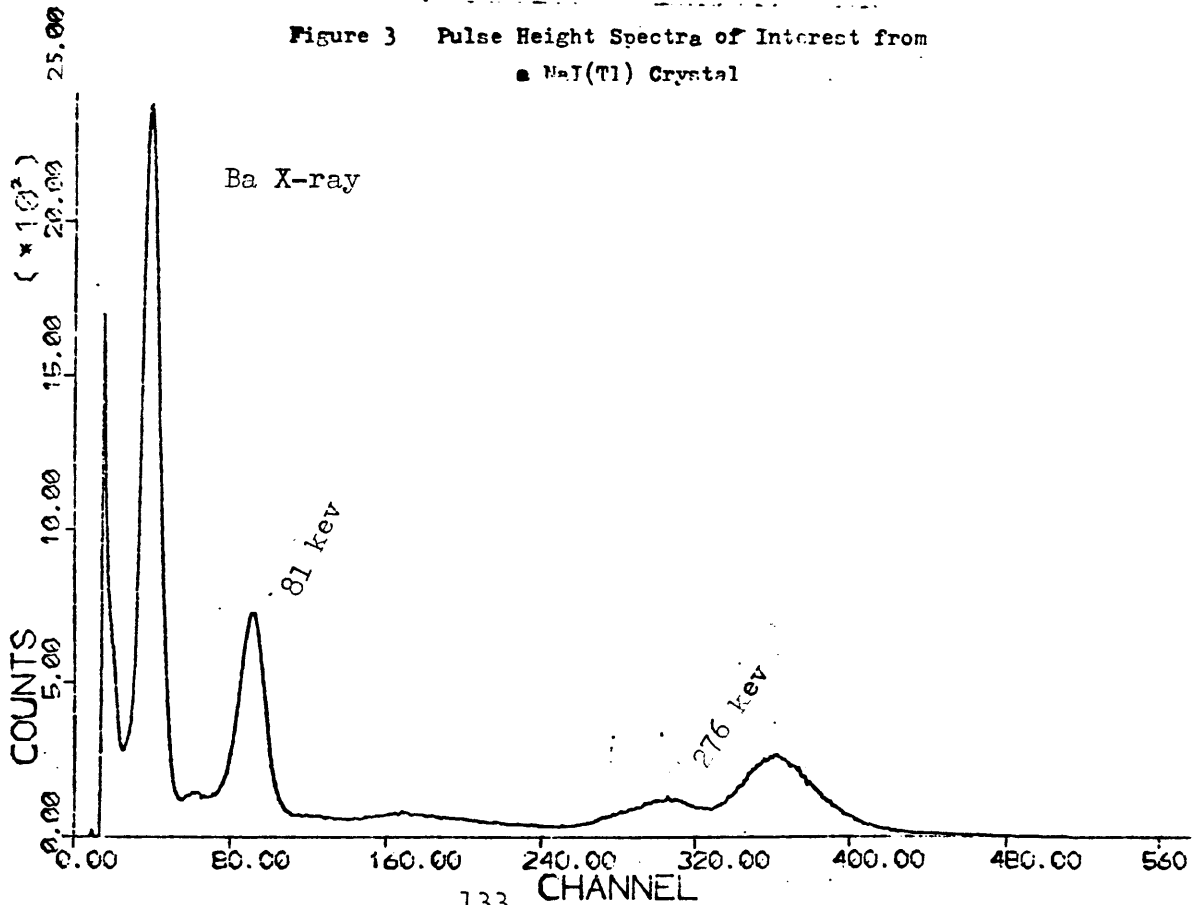
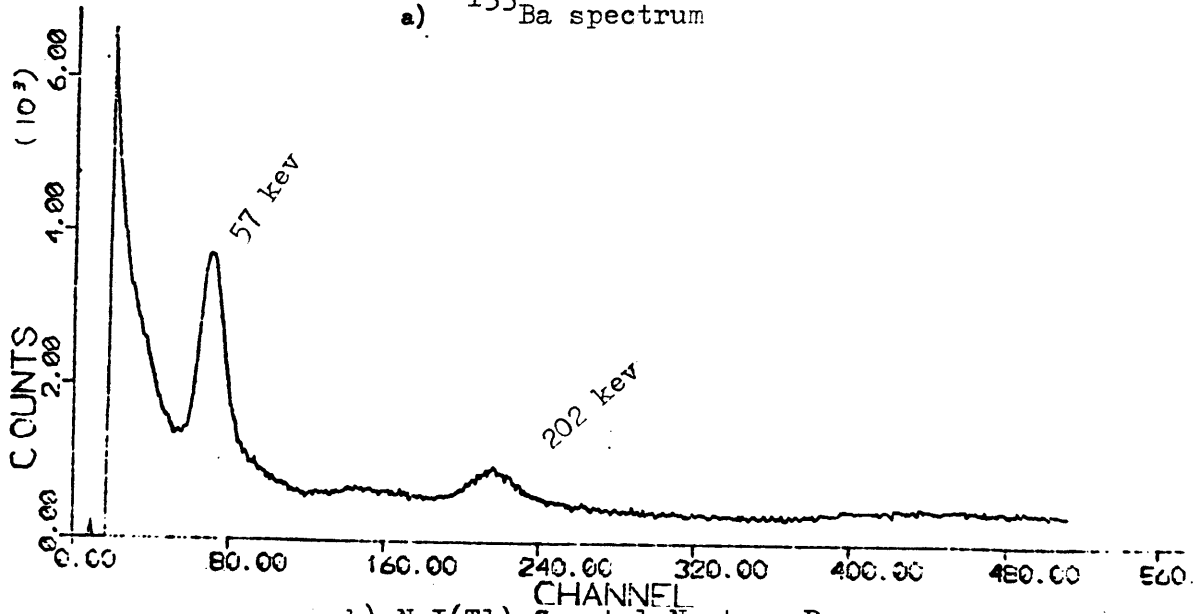


Figure 2
 Level Diagrams for the Lowest Levels of ^{127}I and ^{23}Na
 The arrows indicate observed transitions and
 the numbers above the indicators are the
 branching ratios.

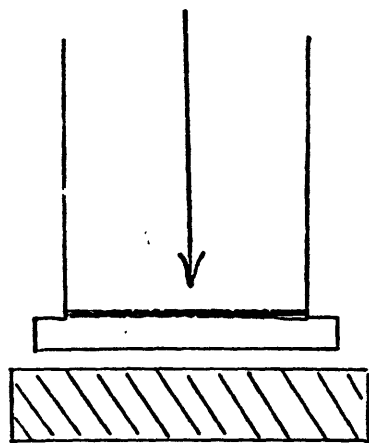
Figure 3 Pulse Height Spectra of Interest from
• NaI(Tl) Crystal



a) ^{133}Ba spectrum



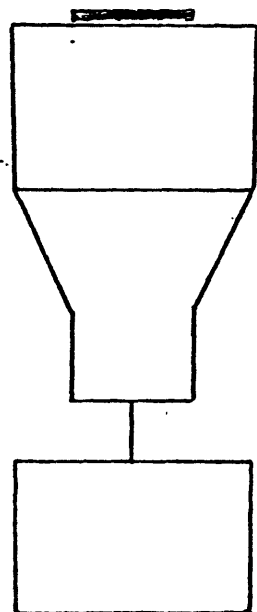
b) NaI(Tl) Crystal Neutron Response



D BEAM

TARGET

X RAY SHIELD



SAMPLE
NaI (TI) CRYSTAL

PHOTO TUBE

MCA

Figure 4 Experimental Set Up

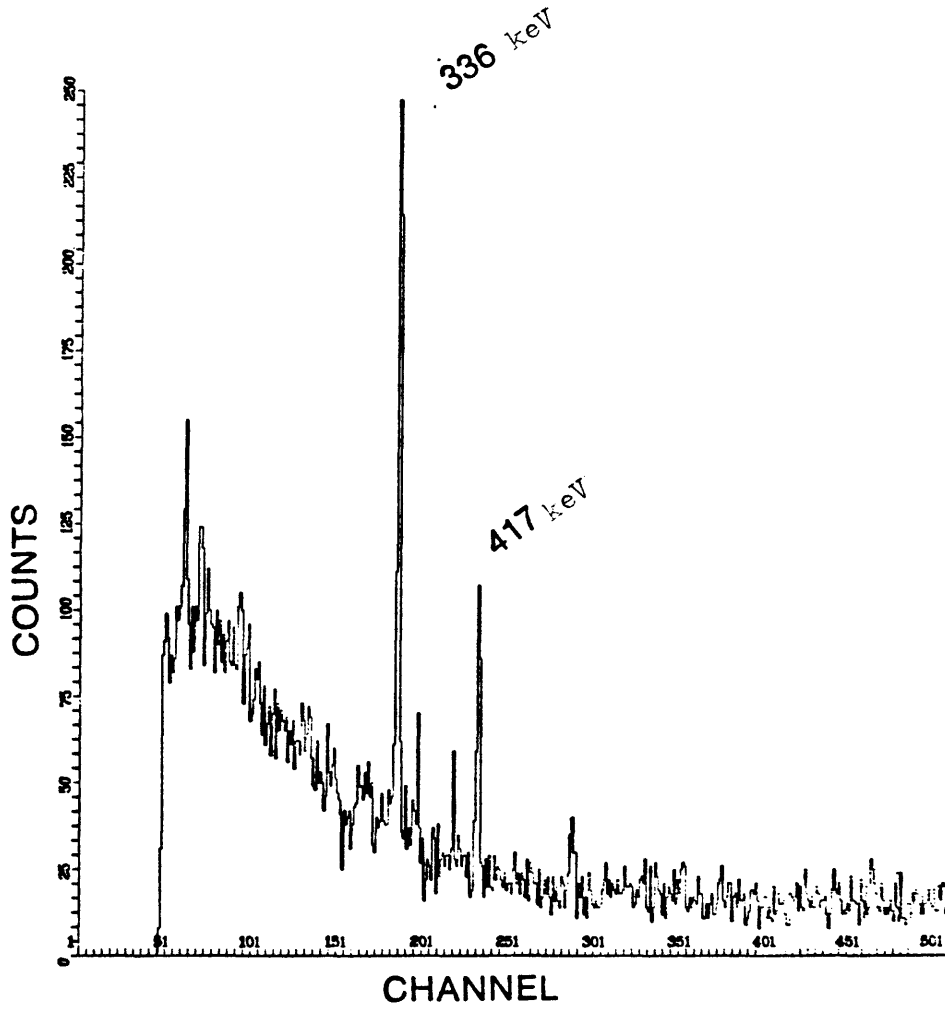


Figure 5 Spectrum of In sample after Neutron Bombardment

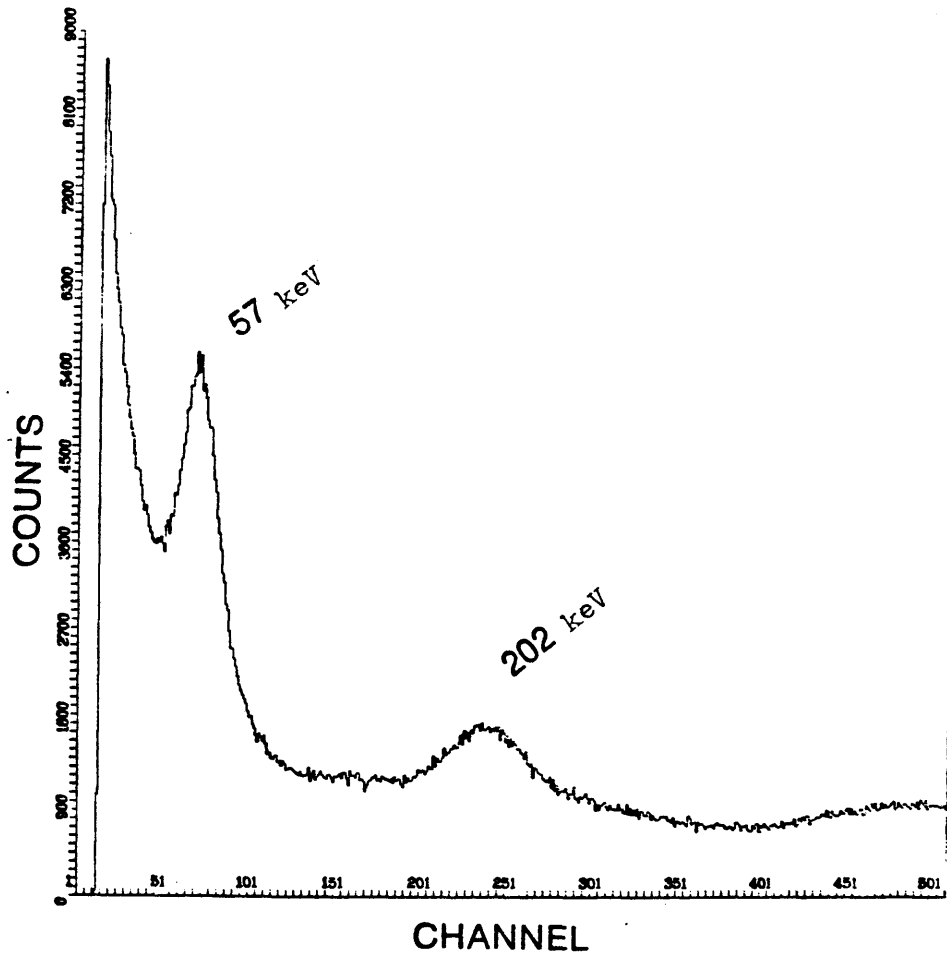


Figure 6 Typical NaI(Tl) Neutron Response
This spectrum shows problems of
a lower resolution crystal.

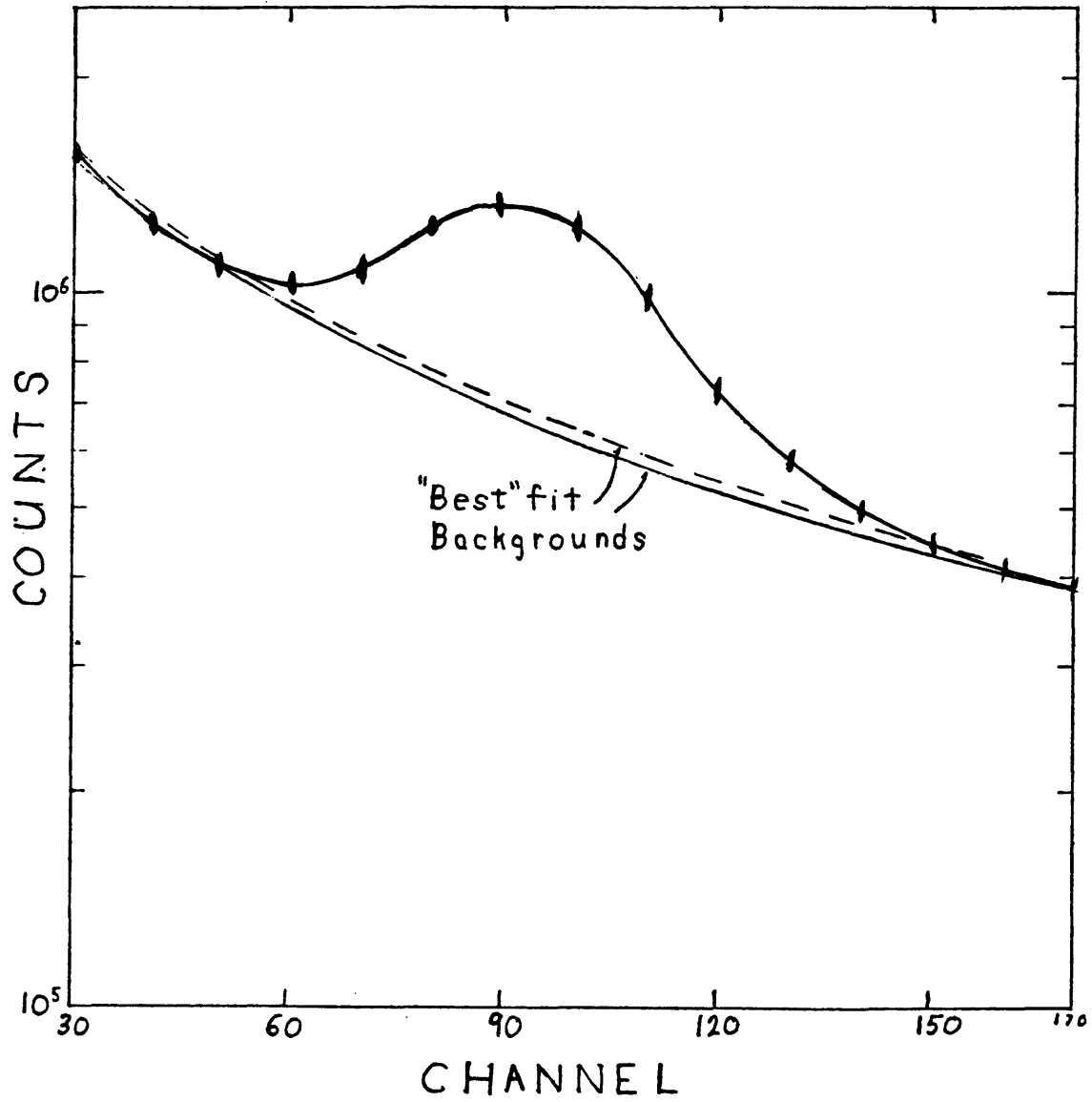


Figure 7
 57 keV Peak and Two "Best Fit" Backgrounds
 The ellipses are centered about the actual data points. The lower lines are the background curves hand fit to determine error.

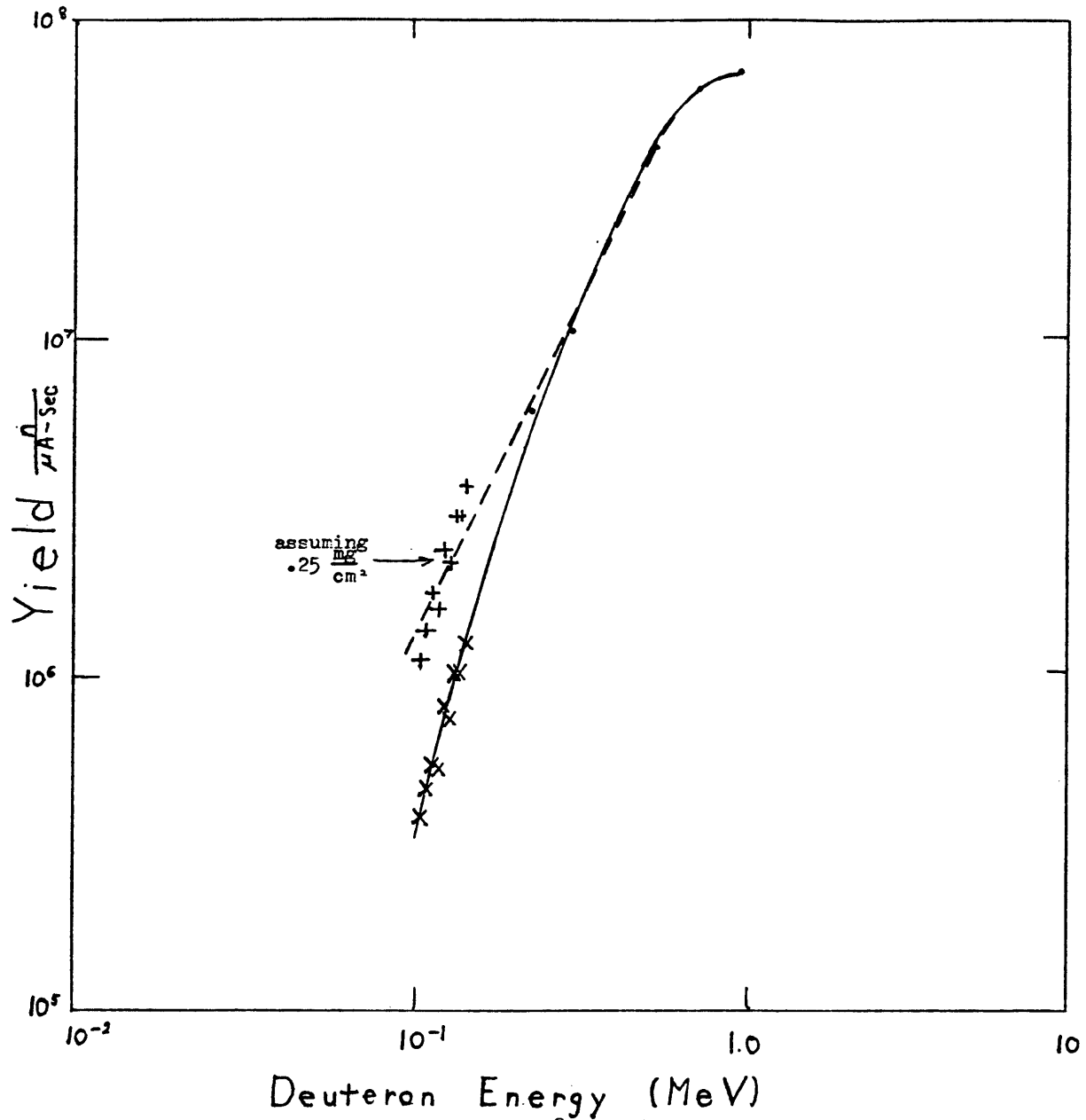


Figure 8

Plot of Deuterated-Titanium Thick Target Neutron Yield (10) and Experimentally Measured Yields.

Dotted line runs through the center of the measured points to the published data while the solid line represents the curve after renormalizing the data.

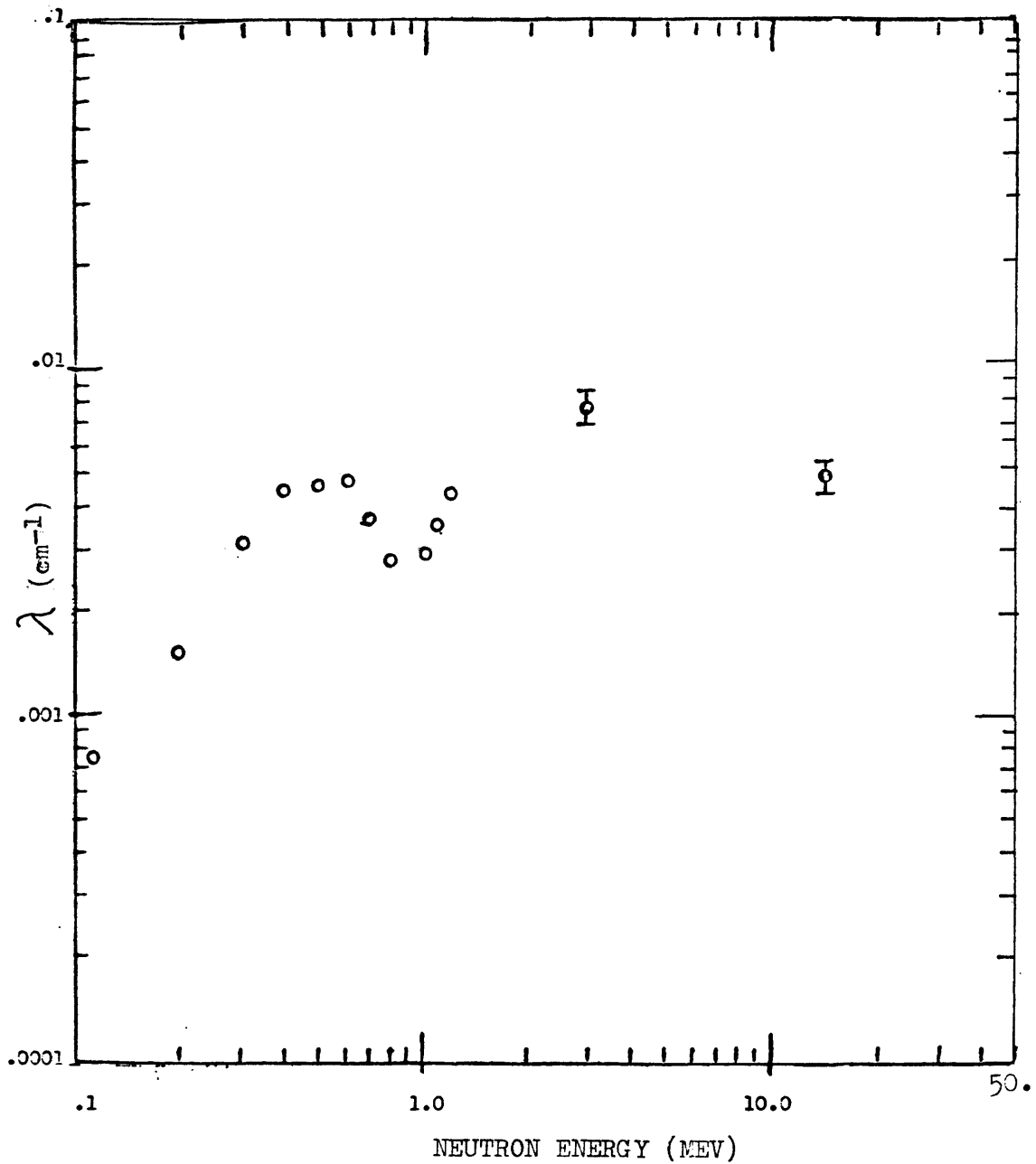


Figure 9
Interaction Length for the Production of the First Excited
State in $I^{27}I$ Circles indicate data from reference (9)
while the solid dots are the present work.

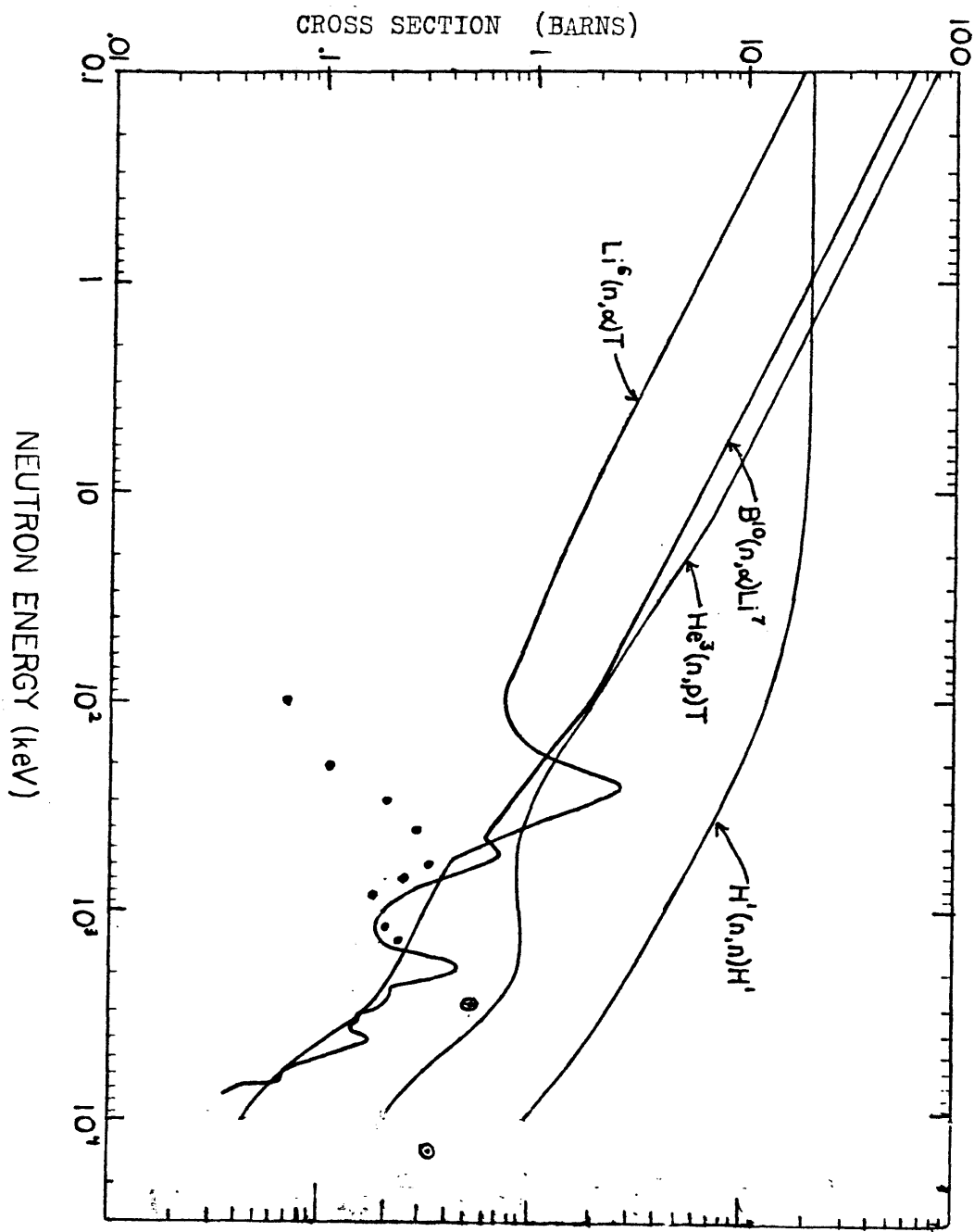


Figure 10
Neutron Cross Sections for Several Reactions Used in Neutron Detection

The curves are measured cross sections (11) for neutron detectors along with data from reference (9) (●) and the present work (⊙) on the $^{127}\text{I}(n, n')$ reaction.

APPENDIX A

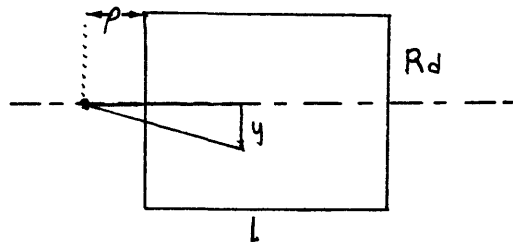
DETECTION EFFICIENCY OF A DETECTOR NEAR A POINT SOURCE

Calculating the detector efficiency for a detector when the geometry is not the plane geometry used in defining the interaction length must be approached on a case by case basis. A common case is a cylindrical detector of radius R_d and length L which is located a distance ρ away from a point particle source.

For the NaI(Tl) neutron detector special circumstances exist in that detection of a neutron does not lead to its removal from the neutron flux. Therefore, assuming the crystal is thin with respect to the neutron absorption length, the number of neutrons detected (N_d) in a length of crystal L is

$$N_d = \lambda L$$

The flux from a point source at a distance r from the source is $N_p/4\pi r^2$, where N_p is the total number of neutrons produced. The r^{-2} dependence of the flux means some of the



neutrons will escape from the sides of the crystal. The number of neutrons detected by the crystal is equal to the integral of the flux passing through the plane a distance r from the source times the length of the crystal traversed by the particles or

$$Nd = \int_0^{R_d} \frac{Np \cdot Lp \cdot \lambda \, da}{4\pi(r+y)^2} = \frac{\lambda Np}{2} \int_0^{R_d} \frac{Lp(y) \cdot y \cdot dy}{(r+y)}$$

The length of the neutron's travel through the crystal Lp is a complex function of y . Simplification is obtained by dividing the crystal into two segments. The first segment is in the solid angle subtended by the back face of the crystal. In this segment

$$Lp = \sqrt{(\rho+L)^2 + y^2} \left(1 - \frac{\rho}{\rho+L}\right)$$

As a result of the crystal being thin, the flux passing through the back face is still given by $1/r$. The integral for the first segment is then:

$$Nd1 = \frac{\lambda \cdot Np \cdot L}{2 \cdot (\rho+L)} \int_0^{R_d} \frac{y \, dy}{\sqrt{(\rho+L)^2 + y^2}} = \frac{Np \cdot L}{2} \left[\sqrt{1 + \left(\frac{R_d}{\rho+L}\right)^2} - 1 \right]$$

The length Ld for the rest of the crystal is :

$$Ld = -\sqrt{\rho^2 + y^2} \left(1 - R_d/y\right)$$

Using the flux on the front face and noting that the minimum y for section 2 on the front face is

$$y_m = \rho \frac{R_d}{\rho+L}$$

thus the number of neutrons detected in section 2, $Nd2$, is

$$Nd_2 = \frac{\lambda \cdot N_p}{2} \int_{y_m}^{R_d} \frac{(R_d - y)}{\sqrt{\rho^2 + y^2}} dy$$

Adding the two pieces together gives a total number of detected neutrons to be

$$N_d = \left[(\rho + L) \sqrt{1 + \left(\frac{R_d}{\rho + L}\right)^2} - L - \rho \sqrt{1 + \left(\frac{R_d}{\rho}\right)^2} + R_d \left(\text{Sinh}^{-1} \left(\frac{R_d}{\rho}\right) - \text{Sinh}^{-1} \left(\frac{R_d}{\rho + L}\right) \right) \right]$$

However if the radius of the detector is assumed to be small then this formula can be simplified to:

$$N_d \approx \frac{\lambda \cdot N_p \cdot R_d^2 \cdot \pi}{4\pi \rho (\rho + L)} \left[1 - \frac{R_d^2}{12L} \frac{(\rho + L)^3 - \rho^3}{\rho^2 (\rho + L)^2} \right]$$

$$= \frac{\lambda \cdot N_p \cdot (Area)}{4\pi \rho (\rho + L)} [1 + C_t] .$$

APPENDIX B

DETERMINATION OF THE EFFICIENCY OF THE GE(LI) DETECTOR

The efficiency of the CSM Ge(Li) detector for the ^{115}In isomeric transition gamma ray was determined using a ^{133}Ba gamma ray source. This source, calibrated by New England Nuclear, had an activity of $1.01 \mu\text{c} \pm 5\%$.

To get acceptable counting errors it was necessary to place the In sample close enough to the detector face so that it subtended a significant solid angle. However, the calibrated source, which consisted of a small amount of Ba in the center of a plastic disk, approximated a point source. Therefore, an averaging technique was used to measure the efficiency for the larger In sample.

The averaging was done by placing the calibrated source a predetermined distance from the face of the detector. Counts were taken with the source aligned with the center of the detector and at several points in the plane of the source. These counts were then compared with the known activity of the source to get the

detector efficiency at each of the test points:

The Indium sample was octagonal in shape. Assuming that the octagon could be represented by a circle and the detection efficiency has a linear correction with the distance from the detector's center line, the detection efficiency for the sample should be equal to the efficiency at two thirds the samples radius. The data from the six test points at this radius were averaged to give a total efficiency. This result was checked by averaging the efficiencies for the points at the center of each of the octagon's quarters, and was found to be identical to the previous result of 1.33%.

References

1. W.W. Givens, W.R. Mills, C.L. Denvis, and R.L. Caldwell, "Uranium Assay Logging Using a Pulsed 14-MeV Neutron Source and Detection of Delayed Fission Neutrons," *Geophysics*, 41, 468-490 (1976).
2. D.A. Lind, R.E. Bently, J.D. Carlson, S.D. Schery, and C.D. Zafiratas, "A Cyclotron Neutron Time-of-Flight Facility", *Nuclear Instruments and Methods*, 130, 93-103, (1975).
3. EG&G Ortec "Radiation and Analysis Instruments for Research and Industry", Physical Sciences Division Ortec Inc, Catalog 1004, p47,(1976).
4. C.M. Lederer, J.M. Hollander, and I. Perlman, "Table of Isotopes," John Wiley and Sons, (1968)
5. J.B. Marion and F.C. Young, "Nuclear Reaction Analysis", North Holland Publishing Company, Amsterdam, p63.
6. I. Bergqvist and B. Lundberg, "Gamma-Ray Spectra from Inelastic Neutron Scattering", *Nuclear Physics*, 80, 198-208, (1966).
7. C.A.R. Bain and F.D. Brosks, "Inelastic Scattering of Neutrons to the 59 keV Level of ^{127}I ", *Nuclear Physics*, A125 312-320 (1956).
8. J.B. Guernsey and A. Wattenburg, "Excitation of Some Low-Lying Levels by Inelastic Neutron Scattering", *Physical Review*, 101 n5, 1516-1523, (1956).
9. J. VanLoef and D.A. Lind, "measurement of Inelastic Scattering Cross Sections for Fast Neutrons", *Physical Review*,

References cont.

9. (cont.) 101, 103-113, (1956).
10. S. Nargolwalla and E. Prxybylowics, "Activation Analysis with Neutron Generators", John Wily and Sons, New York, (1968), p125.
11. J.E. Marion and F.C. Young, op.cit., p125.